Engineering Properties of Soft Rock with High Geostress and the Performance Under Excavation of Deep Tunnel

Yingdong Pan[1] · Heng Zhang[1] · Zihan Hao[1] · Gang Zhang[1] · Shougen Chen[1] · Lu Wang[2]

Abstract

The large deformation of soft rock is one of the most prominent problems in the deep tunnel during excavation, which brings serious potential safety hazards and economic losses. Understanding the deformation mechanism of soft rock is the key to resolving the large deformation issue. In this study, a series of physical and chemical experiments and mechanical experiments were conducted to examine the engineering properties of soft rock. In addition, field monitoring tests are implemented to observe the performance of soft rock during tunnel excavation. Through analyzing the deformation mechanism and law of soft rock, the relationship between the engineering properties of soft rock and performance under excavation of deep tunnel was established. The results showed that free swell rate of the rock samples is $10 \sim 25\%$, and the average swell force is 11 kPa, which indicated that the soft rock has a weak swell force. The mechanical properties of soft rocks such as the peak strength and elastic modulus under different confining pressures are also obtained. The results of field monitoring showed soft rock has a rapid short-term deformation and a slow long-term deformation property, and its short-term deformation even reaches $10 \sim 20$ cm. In addition, the phenomenon of cross section shrinkage is prominent when tunnel passes the section of soft rock. The damage modes of soft rock tunnels can be classified as shotcrete layer fracture, steel arch distortion, collapse at the face. Moreover, some measures and suggestions are proposed to deal with the large deformation problem.

1 Introduction

With the rapid development of China's infrastructure, all kinds of tunnel projects such as traffic tunnels, hydraulic tunnels, and mining tunnels have been constructed or under construction, which provides great convenience and benefits for the public [1–6]. Meanwhile, the increase in the number of long, large-span and deep tunnels has also brought a series of new problems and challenges, among which large deformation of the soft rock mass is one of the most significant problems [7–13]. When a deep tunnel passes through soft

✉ Heng Zhang
  tunnelzh@home.swjtu.edu.cn

✉ Gang Zhang
  zg19970521@my.swjtu.edu.cn

[1] Key Laboratory of Transportation Tunnel Engineering, Ministry of Education, Southwest Jiaotong University, Chengdu 610031, Sichuan, China

[2] Department of Road and Bridge Engineering, Sichuan Vocational and Technical College of Communications, Chengdu 611130, Sichuan, China

rock section, the large deformation could happen and result in cross section shrinkage, lining cracking, shotcrete spalling, steel arch distortion, etc. [14–20], which not only causes economic losses and construction delays, but also endangers the lives of construction workers. Therefore, the large deformation of soft rock has been an increasing concern for deep tunnels in these years.

The International Society for Rock Mechanics (ISRM) first described the rock with an UCS (uniaxial/compressive strength) in the range of 0.25–25 MPa as the soft rock [21]. However, some scholars [22, 23] found if the rock is under the geostress of more than 25 MPa, it may also show the mechanical characteristics of soft rock. So, He et al. [24] proposed a concept of engineering soft rock referring to the rocks that can produce significant plastic deformation under engineering forces. The concept of engineering soft rock emphasizes the importance of strength characteristics and the engineering forces, using the following conditions:

$$\begin{cases} \sigma \geq [\sigma] \\ U \geq [U] \end{cases} \quad (1)$$

where σ is the engineering stress (MPa), $[\sigma]$ is the strength of engineering rock mass (MPa), U is the rock deformation (mm), and $[U]$ is the deformation allowance (mm).

The engineering properties of rock have a close relationship with mineral composition, rock structure, groundwater, weathering factors, etc. [25–30]. Zhang [31] pointed out that the mineral composition and structure of rock are important factors affecting its mechanical properties and the uniaxial compressive strength and elastic modulus of the rocks will increase due to the content of quartz. Based on mineral composition detection and microstructure observation, Bian et al. [32] illustrated the reasons for the decrease in strength and deforming resistance of tunnel rock masses after water infiltration. Lin et al. [33] determined the rock mineral composition by X-ray diffraction analysis, and by observing the rock microstructure with scanning electron microscopy (SEM), they pointed that the feldspar will increase rock brittle and the increment of calcite content will reduce the compressive strength and elastic modulus of rock. Li et al. [34] analyzed the influence of mica content, particle shape and size, cracks and porosity in the rock and other factors on the rock engineering properties. However, due to the particularity of soft rock tunnels, literature related to physical and chemical experiments of soft rock is not much.

The large deformation of soft rock is caused due to the instability of ultimate shear stress [35], and it usually occurs around the excavation surface of underground space. And the large deformation is a time-dependent behavior and it could last a very long time [36]. Many scholars have conducted to study the failure mechanism of soft rock and the law of deformation [37]. Chen et al. [38] proposed that the mechanism of convergence deformation of surrounding rock should include five aspects: plastic wedge, flow deformation, swelling, dilatation and deflection of the surrounding rock. Anagnostou [39] thought that large deformation mainly depends on rock strength and overburden thickness, and it can occur in any type of rock mass. Singh et al. [19] pointed out that large deformation occurs on the premise of weak surrounding rock combined with high in-situ stress. Jiang et al. [40] proposed a theoretical method for predicting the development of a plastic zone and loosening pressure in soft rock tunnels and discussed the influence of the mechanical properties of soft rock on loosening pressure. In addition, Chu [41] et al. derived an analytical solution for lined circular tunnels in deep viscoelastic burgers rock, which considers various factors such as excavation methods, rheological rocks, and supporting forms. With respect to countermeasures for large deformation, Goel et al. [42] introduced the Maneri-Uttarkashi power tunnel passing through the chlorite schist, and the support scheme includes adding invert struts, removing and replacing steel arch, strengthening pre-support and grouting reinforcement. However, previous support theories and traditional technologies cannot effectively control soft rock deformation in some deep tunnels [43], and new support technologies have been developed, including retractable support [44] and bolt-net-cable coupling support [45, 46]. Additionally, Yassaghi et al. [47] emphasized the importance of proper and timely support to prevent the large deformation of soft rock in tunnel engineering.

However, there is little literature about the relationship between the engineering properties of soft rock and the performance under the excavation of deep tunnels. This study is based on the construction project of headrace tunnels of Jinping II Hydropower Station. A series of physical and chemical experiments and mechanical experiments were conducted to examine the engineering properties of soft rock. In addition, field monitoring tests are implemented to observe the performance of soft rock during tunnel excavation. Through analyzing the deformation mechanism and law of soft rock, the relationship between the engineering properties of soft rock and performance under excavation of deep tunnels was established. The findings can provide valuable reference data for addressing the problem of large deformation of soft rock in deep tunnels.

2 Engineering Background

The Jinping II Hydropower Station, the world's largest underground complex, is located on the trunk stream of the Yalong River in Liangshan Prefecture, Sichuan Province, China. The hydroelectric station consists of seven tunnels (including four headrace tunnels, two traffic tunnels, one drainage tunnel), a river sluice on the west side of Jinping Mountain and an underground powerhouse on the east side of the mountain. Harnessing the hydraulic head of 310 m of Jinping Bend of the Yalong River, the hydropower station generates electrical energy by diverting water into headrace tunnels through Jinping Mountains, as shown in Fig. 1.

In the tunnel system of the Jinping II Hydropower Station, as shown in Fig. 2, there are four parallel headrace tunnels of which the length is 16.7 km, the space is 60 m, the diameter is 12.4 ~ 13 m, and the gradient is 0.365%. The average depth of four headrace tunnels is 1500 ~ 2000 m, and the maximum is 2525 m, which means that it even exceeds the world's deepest railway tunnel—the Gotthard Base tunnel (the maximum depth of 2450 m) and it is one of the most representative deep tunnel projects.

The headrace tunnels are excavated from the east and the west ends to the middle at the same time by drilling and blasting methods and TBM method. The section of tunnels that adopt the drilling and blasting method is horseshoe-shaped and the lining structure is the reinforced concrete of which the minimum thickness is not less than 50 cm.

The Yalong River valley, at which the hydropower station is located, has a typical V-shaped cross section with steep
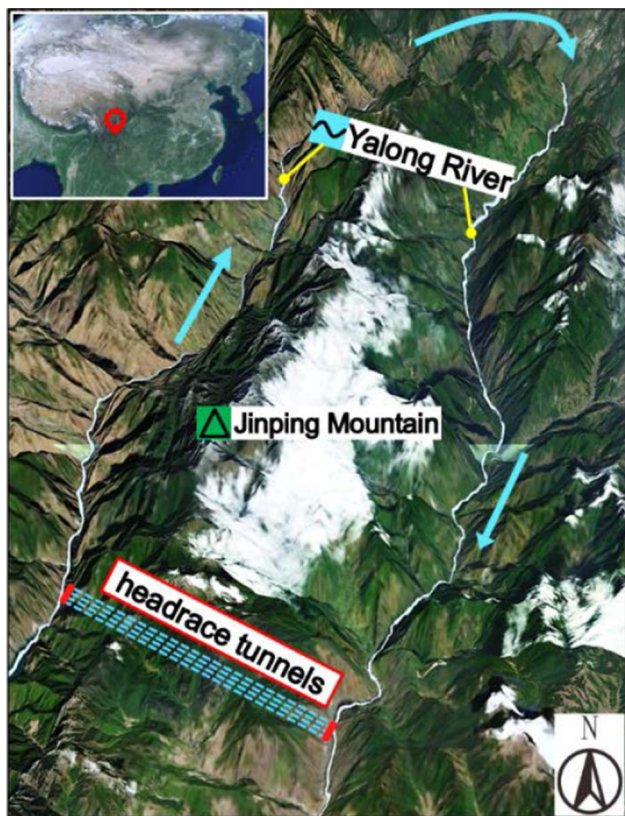
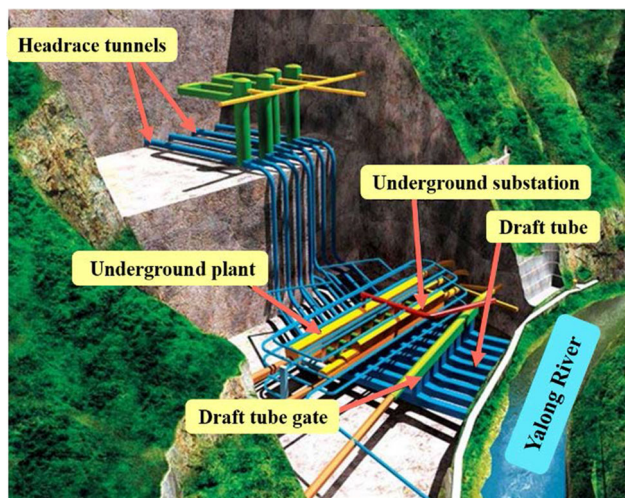Fig. 1 The location of Jinping II hydropower station

Fig. 2 The 3D designed drawing of Jinping II hydropower station

slopes on both sides. The elevations of the mountains are more than 3000 m, and the highest peak reaches 4125 m. The terrains on both sides of the watershed are asymmetrical, and the east side is wide and the west side is narrow. In the foothills and gullies, there are a lot of collapse deposits and debris cones, which form alluvial cones. High mountain, deep valley and steep slope are the topographical features of the engineering zone.

The rock stratums, in which the headrace tunnels are constructed, consist of Lower Triassic chlorite schist (T1), Middle Triassic Zagunao Formation (T2z), Upper Triassic sand slate (T3), Middle Triassic Baishan Formation marble (T2b) and Middle Triassic Yantang Formation marble (T2y) from west to east, as shown in Fig. 3.

According to the signs of the geological structure in Jinping Bend, the engineering zone is under the control of the approximately east–west (NWW ~ SEE) stress field, which causes a series of south-north trending compact folds and high-angle faults under compression or compression-torsion.

Due to the chlorite schist formation acting as a water-resistant layer, the fissure water in the headrace tunnels is not well developed, and only a small amount of drops can be seen, and continuous drops can be noticed occasionally.

3 Engineering Properties of Soft Rock

3.1 Physical and Chemical Properties

To investigate the swelling properties, the microstructure and mineral composition laboratory tests including the swelling test, XRD and SEM were performed.

3.1.1 SEM–EDS Test

Four groups of rock samples (I, II, III, V) were used for the laboratory tests. The four groups of samples were collected from four places which are at 1 550 m,1 650 m from the entrance of #1 headrace tunnel and 1 620 m, 1 640 m from the entrance of #2 headrace tunnel, as shown in Figs. 4 and 5.

In order to analyze the microstructural characteristics and the elemental composition of soft rock, an SEM–EDS test was conducted using a Philips Quant-200 type SEM equipped with an EDS system at Key Laboratory of Advanced Technologies of Materials of Southwest Jiaotong University, as shown in Fig. 6.

The SEM images showed rough surfaces of rock samples, fine flake structure (typical characteristics of chlorite) and sheet structure packed with detrital particles. It may be inferred that the soft rock contacts water once, the weathered detritus from the parent rock float in the water and the contact forces between the parent rock particles are reduced greatly, and the strength of the rock mass decreases rapidly.

In order to analyze local characteristics of the structure, it can be seen from Fig. 7 that there is a relatively complete crystal structure with surface-to-surface contacts between the microstructural units. Based on the morphology and distribution of the detrital particles in the figure, it can be inferred that the crystal structure of the rock sample is easily destroyed or
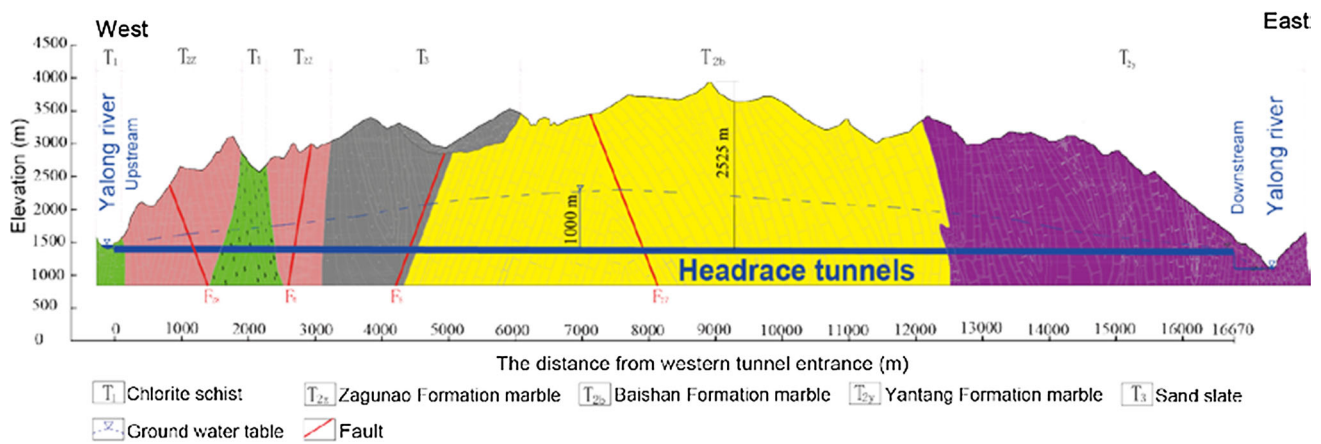
Fig. 3 Geological structures and lithology of Jinping Mountain

Fig. 4 The geological condition exposed

Fig. 5 Rock samples

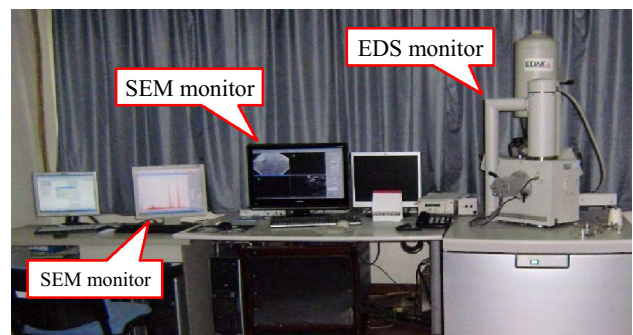weathered, forming detrital particles distributed uniformly on the surfaces of rocks.


Fig. 6 The SEM–EDS system

The EDS spectrum shows that the chemical elements of the soft rock include O, Si, Mg, Ca, Fe, Al, Au. According to the previous geological survey, the soft rock is chlorite schist of which main component is chlorite. The chlorite is composed of silica and silicate, and its major elements are O, Si, Mg, Fe, Al, along with minor other elements such as Ca, Ti, Mn, and Cr. Therefore, the results of EDS tests agree with the conclusion from the previous geological investigation.

3.1.2 XRD Test

X-ray powder diffraction (XRD) is an effective analytical technique used for identifying mineralogical compositions and contents of rock samples. This study used a PANalytical XRD instrument at Key Laboratory of Advanced Technologies of Materials of Southwest Jiaotong University, as shown in Fig. 8. Four groups of rock samples were first crushed to fine powder using an agate mortar and pestle. Next, the powder was collected in a glass container, and then used for XRD analysis. The XRD test is conducted at 40 kV and 40 mA with the scan speed of 0.1 s/step, the sampling step width of 0.01° 2θ, and the scan range from 0° to 100° 2θ.
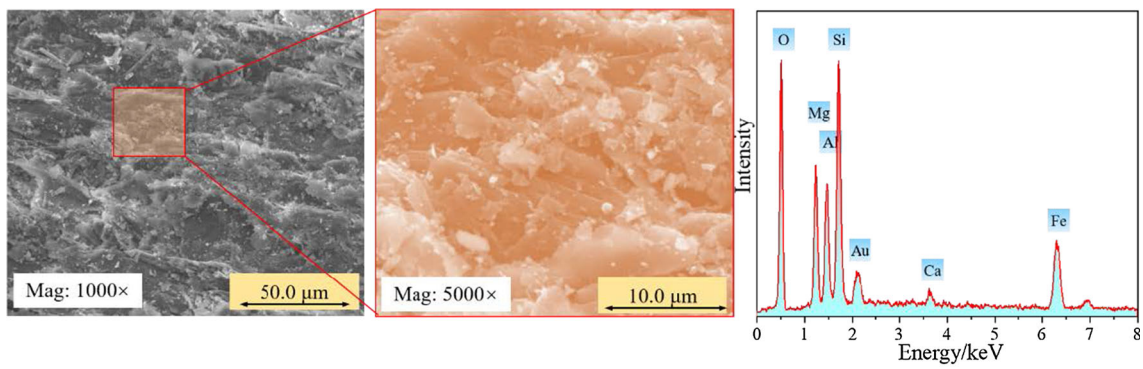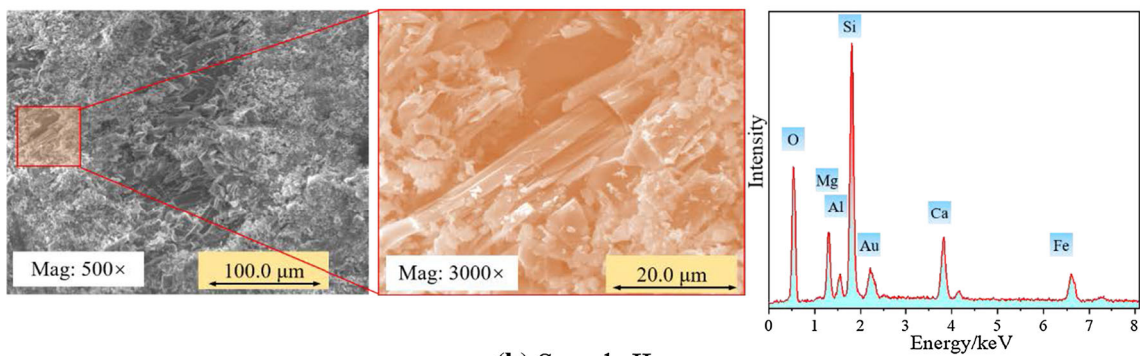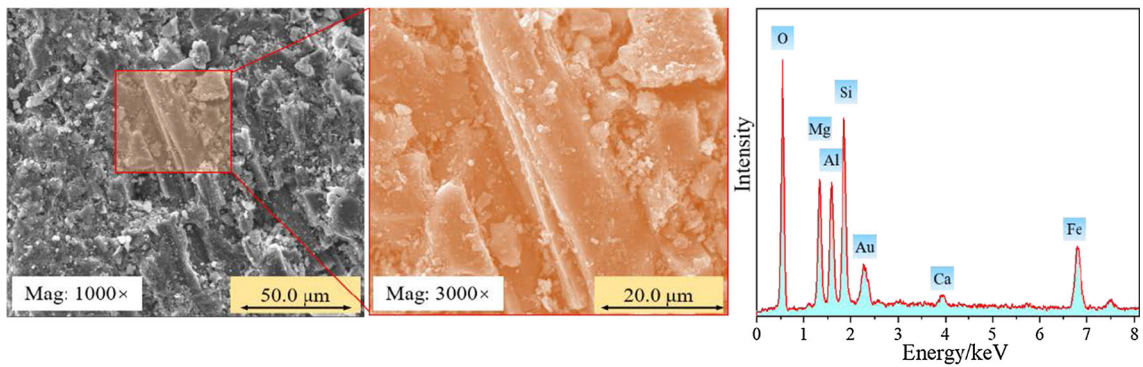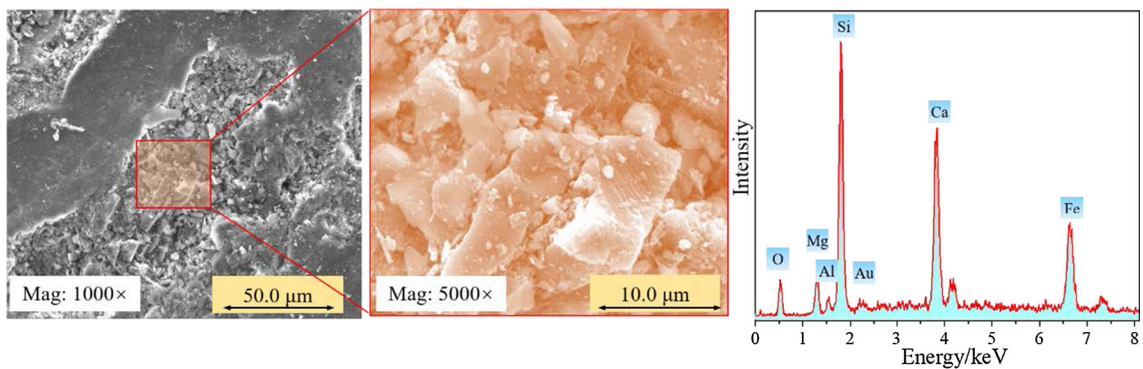
Fig. 7 SEM–EDS images of chlorite schist

Fig. 8 XRD system

(a) XRD instrument   **(b)** XRD monitor
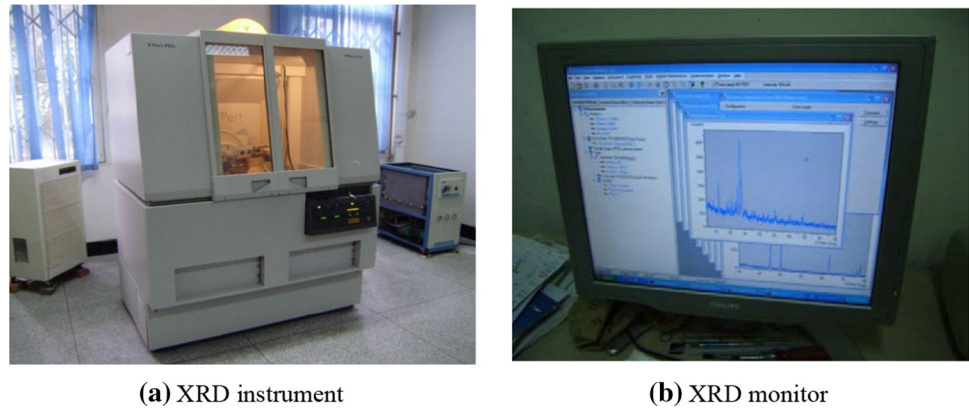
Table 1 Mineral composition of soft rock

No.	Mineral species and content/%								
	Chlorite	Talcum	Amphibole	Calcite	Sericite	Quartz	Epidote	Plagioclase	Albite
I	47.2	8.5	9.7	2.6	6.7	4.6	2.8	1.2	0.9
II	38.9	16.1	10.2	3.3	5.8	6.9	3.4	0.9	0.5
III	44.6	6.2	3.8	4.2	9.5	3.7	1.5	2.0	1.1
IV	41.7	11.3	1.9	6.6	2.8	4.3	4.1	1.5	0.8

As shown in Table.1, the XRD analysis reveals that the major mineral of samples is chlorite (41.7~47.2%), which is easy to soften in water and has thin sheet structure, low strength and relatively strong plastic deformation ability. The results are in good consistent with SEM–EDS analysis. The hydrophilic minerals such as quartz (3.7~6.9%), sericite (2.8~9.5%) make up a considerable proportion, which means that the rock has a strong softening property. And the auxiliary minerals of samples include talcum (6.2~16.1%), amphibole (1.9~10.2%), calcite (2.6~6.6%), epidote (1.5~4.1%), plagioclase (0.9~2.0%), and albite (0.5~1.1%).

3.1.3 Swelling Property Test

In order to study the influence of the swell property of surrounding rock on the deformation, a series of swell property tests were carried out determining free swell rate and swell force, as shown in Figs. 9 and 10.

Table 2 shows that the free swell rate of the rock samples is 10~25%, and the changes of volume have been over within 2 h and remain stable. And the results of swell forces of the four rock samples are 11 k Pa, 9.33 kPa, 7 kPa, 14.27 kPa, respectively. In summary, both free swell rate tests and swell force tests indicate that the rock has a very low swell force. So, it can be inferred that the effect of swell property of the rock is not the controlling factor of large deformation.

3.2 Mechanical Properties

In this study, uniaxial tests and triaxial tests were carried out to study the mechanical properties of chlorite schist under dry and saturated conditions, which mainly include deformation characteristics, strength characteristics, failure modes and the influence of water content (Figs. 11 and 12).
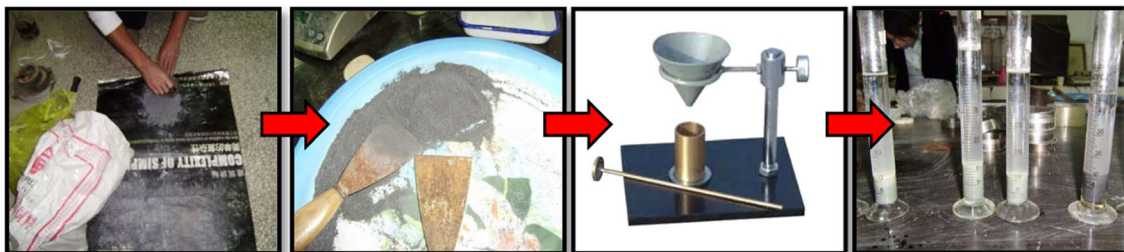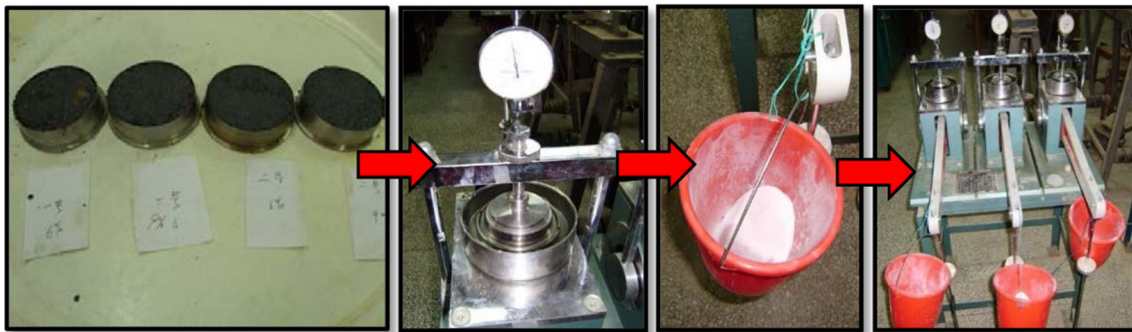

Fig. 9 Free swell rate test

Fig. 10 Swell force test

Table 2 Free swell rate test data sheet

Group	No.	Dry rock mass (g)	The volume at different times (ml)						Free swell rate δ_{ef} (%)
			2 h	4 h	6 h	8 h	10 h	12 h	
I	1	9.48	20	20	20	20	20	20	20
	2	9.52	20	20	20	20	20	20	
II	1	9.53	10	10	10	10	10	10	11
	2	9.49	12	12	12	12	12	12	
III	1	9.75	34	34	34	34	34	34	25
	2	9.72	21	21	21	21	21	21	
IV	1	10.74	13	13	13	13	13	13	23
	2	10.79	13	13	13	13	13	13	

3.2.1 Uniaxial Compression Test

The results of the uniaxial compression tests are exhibited in Fig. 13. The loading behaviors of the rocks in dry state and saturated state are similar, and the two curves both have an obvious compaction stage at the beginning of loading, and then they enter an elastic deformation stage as the loading continues. Before reaching the peak strength, there does not appear to be compaction stage. Finally, the stress–strain curve shows a sudden drop from the peak value.

3.2.2 Triaxial Compression Test

As shown in Fig. 14, the peak stress and the residual stress increase with the confining pressure. After the peak stress, the higher stress shows a slower and less decline, ultimately tending to the ideal plastic deformation state. The above phenomenon indicated that the chlorite schists are sensitive to confining pressure, and have an obvious strain hardening property.

Under dry and saturated conditions, the relationship between peak strength and confining pressure is shown in Fig. 15, which agrees well with the linear characteristics of the Mohr–Coulomb strength criterion. The results showed that the cohesive force c of chlorite schist is 13.74 MPa and the friction angle φ is 21.43° under dry conditions, while

Fig. 11 A rock sample

the cohesive force c is 4.47 MPa and the friction angle φ is 25.26° under saturation condition.

The difference between peak strength and residual strength is called as peak-residual strength. The relationship between peak-residual strength and confining pressure for soft rock is shown in Fig. 16. With the increase of confining pressure, the peak-residual gradually decreases; in other words, the increase of residual strength is larger than the peak

Fig. 12 The triaxial compression apparatus

strength under confining pressure, which means the residual strength of the soft rock is more sensitive than the peak strength.

The relation between elastic modulus and confining pressure for dry and saturated rock is shown in Fig. 17. Under the dry state, the elastic modulus of chlorite schist shows a direct proportion relationship with confining pressure, which means the structure of rock samples is compacted and presented a more obvious hardening effect with the increase of confining pressure. However, under the saturated state, the elastic modulus has little change with confining pressure, which indicates the softening effect is obvious or the hardening effect is weakened when the chlorite schist contact water.

Failure modes of chlorite schist in the triaxial compression test are shown in Fig. 18. It can be seen from the test results
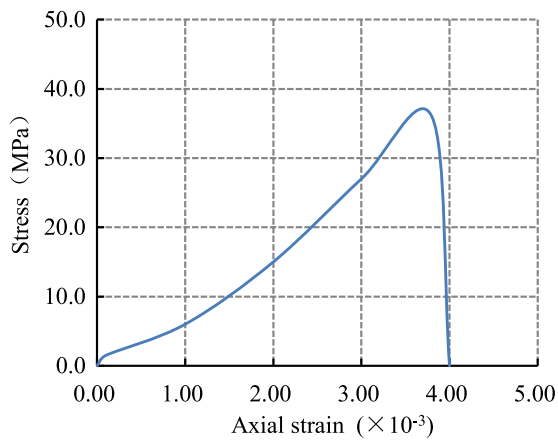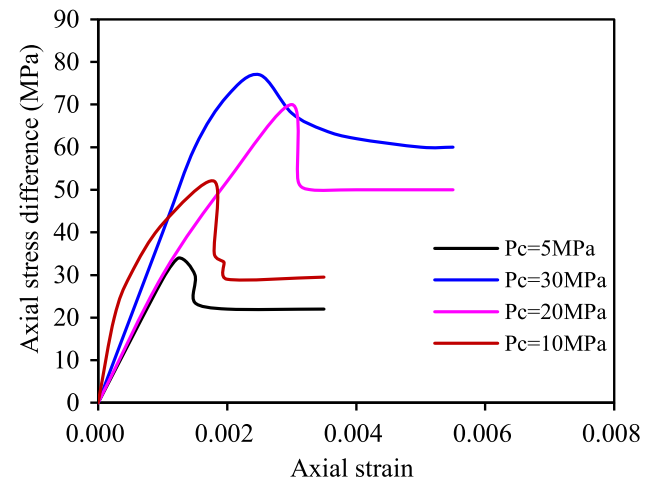

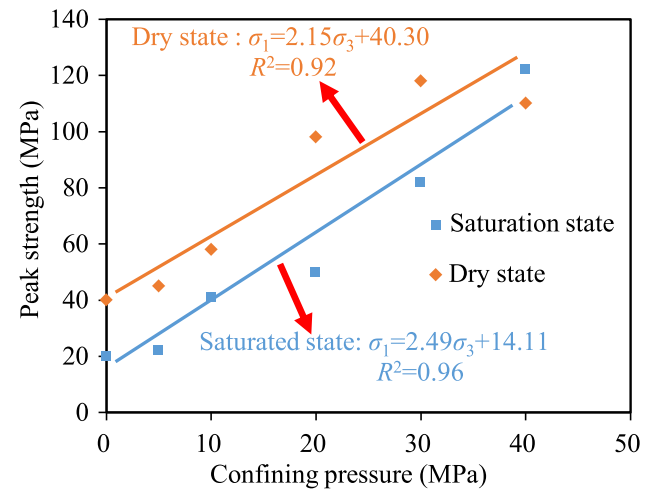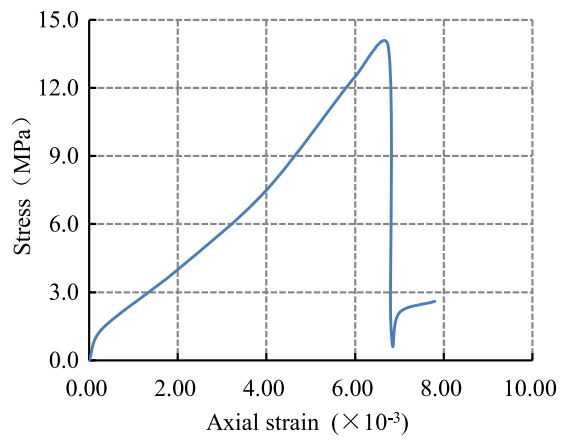**Fig. 14** The stress–strain relationship under different confining pressures

Fig. 15 The relationship between the peak strength and confining pressures

(a) Dry state

(b) Saturated state

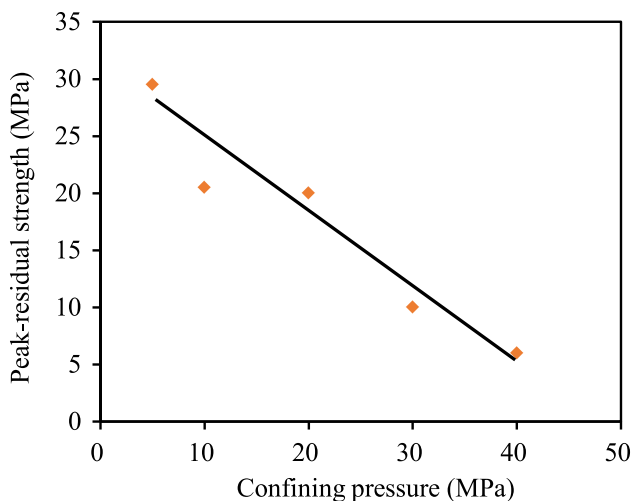**Fig. 13** stress–strain relationship under uniaxial compression

Fig. 16 The relationship between peak-residual strength and confining pressure
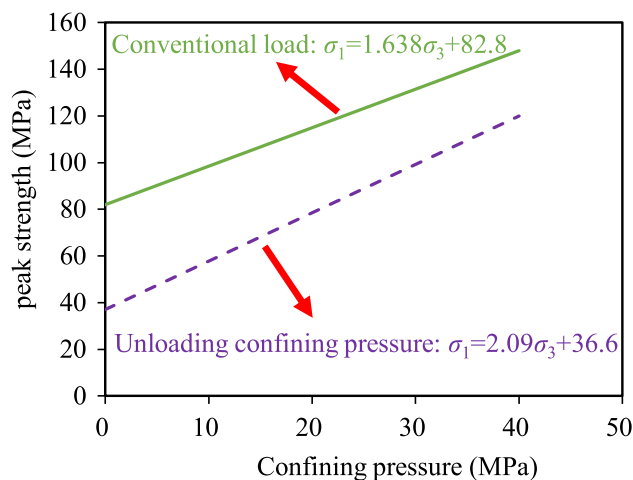

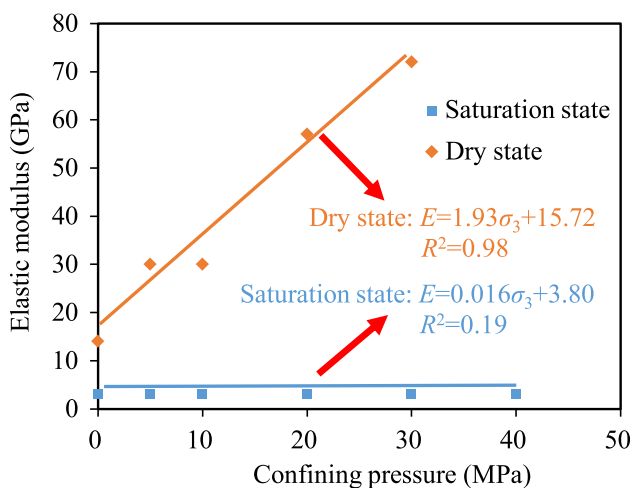**Fig. 19** The peak strength under the condition of loading and unloading

Fig. 17 The relationship between elastic modulus and confining pressure

small fragments appear near the fracture surface. With the increase of confining pressure, the shear surfaces of the sample become more and more smooth, and there is some white powder produced by strong friction on the fracture surface.

In the process of tunnel excavation, the confining pressure actually experiences a stress path of radial unloading and circumferential loading. Deng conducted a triaxial compression test for chlorite schist, and obtained a relationship of peak strength and confining pressure under the conditions of loading and unloading, as shown in Fig. 19. It can be seen from Fig. 19 that the peak strength of unloading is lower than that of loading.

And the percentage reduction, which refers to the proportion of the difference of two loading to the conventional loading, has a relationship with the confining pressure in Fig. 20. According to the descending curve, it can be seen that the percentage decrease of peak strength reaches about 50% at a low confining pressure, while the decrease is 19% when confining pressure rises to 40 MPa. This means the strength of surrounding rock declined significantly after excavation due to the process of unloading and loading; that is to say, the stress state of chlorite schist with low strength after excavation is more unfavorable to bearing capacity.

that the failure modes of the samples under different confining pressures are shear failure. According to the observation of the macroscopic fracture of the rock samples, the fracture surface is rougher at lower confining pressure and many

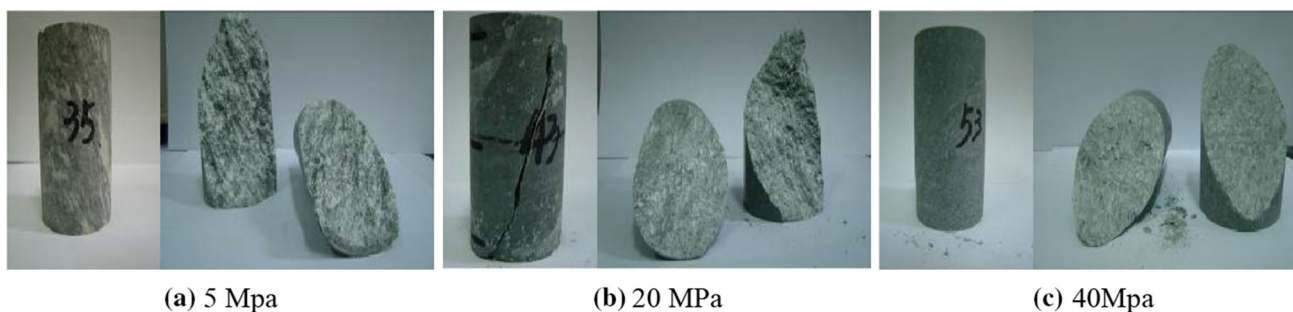**(a) 5 Mpa**　　　　　**(b) 20 MPa**　　　　　**(c) 40Mpa**

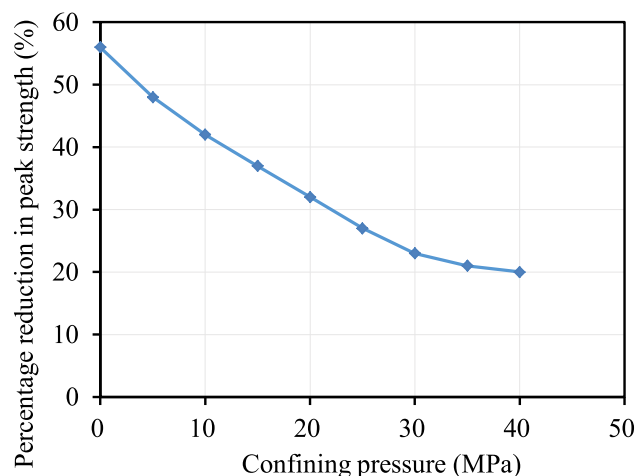**Fig. 18** Failure modes of triaxial compression test

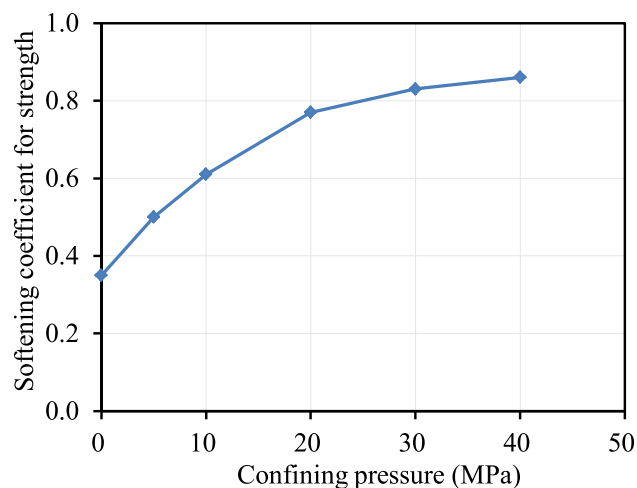Fig. 20 The percentage reduction in peak strength

Fig. 21 The relationship between softening coefficient for strength and confining pressure

Softening coefficient is a representative parameter of water resistance for rocks. In this paper, it is defined as the ratio of compressive strength of rocks saturated with water to that in dry state under the same confining pressure. The relationship between softening coefficient for strength and confining pressure is plotted in Fig. 21. It is noted that the softening coefficient is just 0.38 without confining pressure; that is, the peak strength of the saturated rock sample is about 38% of that of dry rock sample and decreases significantly. Figure 21 also shows that there is a gradual increase in softening coefficient with the increase of confining pressure, which illustrates that softening effect is serious at low confining pressure. It can be inferred that due to low confining pressure, the strength of surface layer of surrounding rock decrease obviously. So, timing preliminary supports can provide reaction force on surrounding rock, reducing the softening effect.
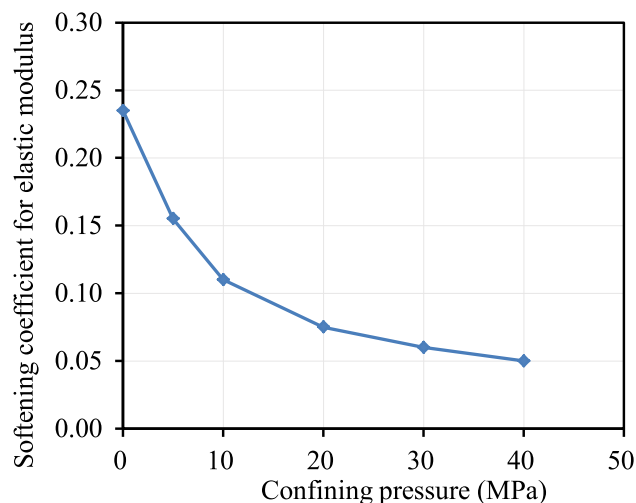

Fig. 22 The relationship between softening coefficient for elastic modulus and confining pressure

The relationship between softening coefficient of elastic modulus and confining pressure is shown in Fig. 22. It can be seen that the softening coefficient is 0.24 without confining pressure; that is, the elastic modulus of saturated rock sample is about 24% of that of dry rock sample. Figure 22 also shows that there is a gradual drop in softening coefficient. This is because the softening coefficient of elastic modulus of dry sample is sensitive to the confining pressure, which leads to softening coefficient decreasing with the increase of the confining pressure. Therefore, the influence of water on the deformation property of chlorite schist is proved to be significant once again.

4 Performance Under Tunnel Excavation

4.1 Convergence Displacement Characteristics

In consideration of the large cross section of headrace tunnels, five measuring points and six measuring lines were set to measure convergence displacements, which can be verified with each other based on triangle law.

According to the results of the convergence displacement measured, it can be seen from Fig. 23 that the surrounding rock shows a rapid short-term deformation and a slow long-term deformation property, and its short-term deformation even reaches 10~20 cm, indicating that the existing support measures are not enough to limit the deformation of surrounding rock and maintain the stability of the tunnel. The results are basically consistent with the actual convex position and crack position on the cross section of the headrace tunnel.
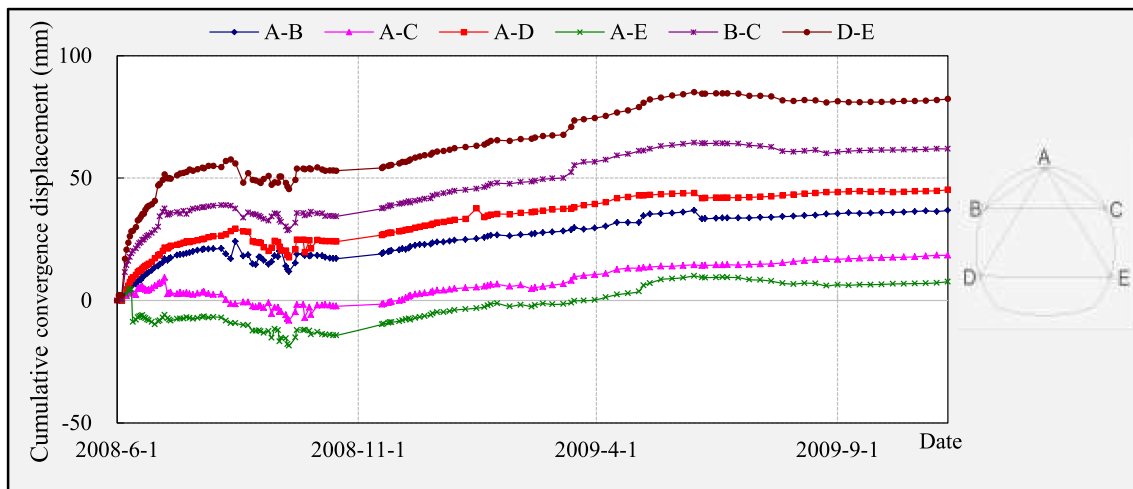
(a) Tunnel #1
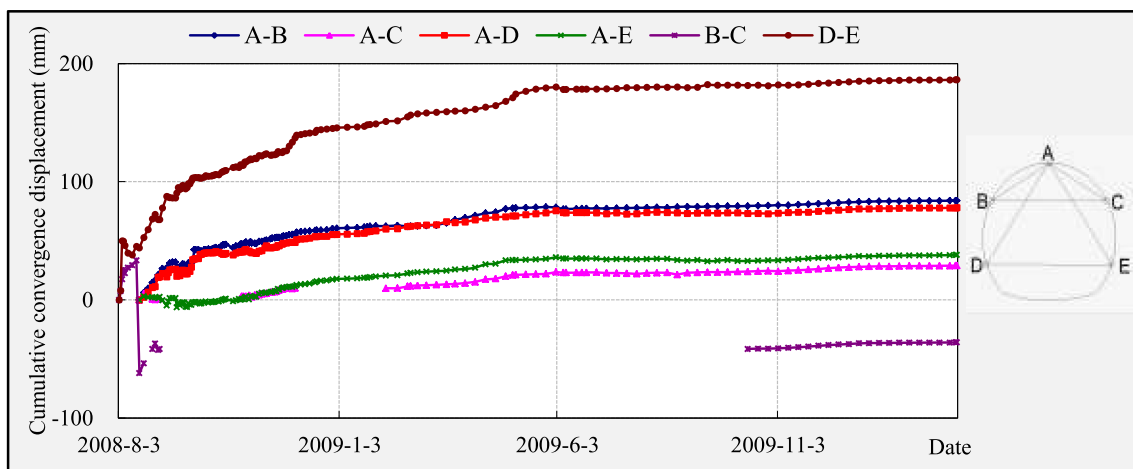
(b) Tunnel #2

Fig. 23 Cumulative convergence displacement (mm)

The position of large deformation on the section is mainly controlled by the stress state, which is ascribed to the plastic flow on the stress concentration region after tunnel excavation. Among all the measuring lines of the convergence displacement, the convergence value of the horizontal measuring lines is larger than that of other measuring lines, and the convergence value of the bottom horizontal measuring line (DE) is largest. This is because before the excavation of the bench, the support structure, steel arch and shotcrete layer, cannot be closed into a ring at the bottom of the side wall, resulting in the lack of constraint on the positions.

4.2 Clearances Deformation Characteristics

After the convergence deformation is basically stable, adopt clearance gauges to measure the clearances deformation of tunnels. 67 cross sections of Tunnel #1 (K1 + 535 ~ K1 + 759 m) and 13 cross sections of Tunnel #2 (K1 + 613 ~ K1 +

643 m) are measured, and the results of the largest deformation of clearance are presented in Fig. 24.

From the above bar graphs, it can be seen that the phenomenon of "shrinkage" is conspicuous in the section of soft rock, and most deformations of surrounding rock exceed the tunnel clearance by 20 ~ 60 cm. And the most prominent deformation problem happened in Tunnel #1 (K1 + 624 ~ K1 + 759 m) and Tunnel #2 (K1 + 614 ~ K1 + 643 m), in which a few deformations are even more than 100 cm.

The statistics on largest deformation positions on the cross section for tunnel #1 and tunnel #2 are shown in Fig. 25. The polar diameter in the graph represents the percentage of the number of the largest deformation sections in the total number, and the angle represents the positions on cross section of tunnel. For Tunnel #1, the largest deformation mainly occurred in the left sidewall, vault and right arc foot, whereas for Tunnel #2, the largest deformation mostly occurred in the vault.
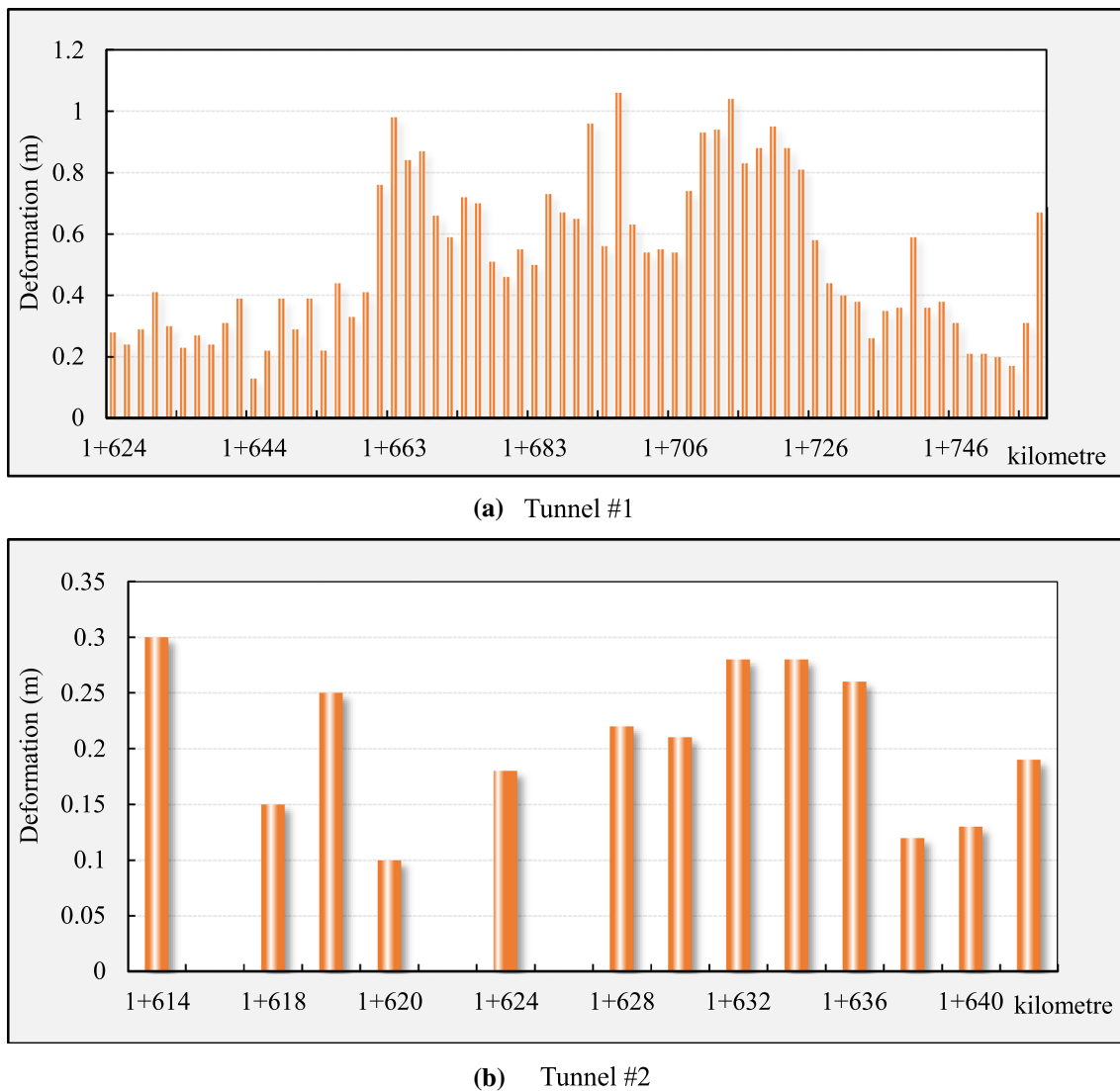
(a)   Tunnel #1

(b)   Tunnel #2

Fig. 24 The largest deformation for tunnel clearance

4.3 Stress–Strain Characteristic

For soft rock tunnels, the deformation adjustment and stress redistribution of the surrounding rock will occur in a period of time after excavation. This study used multi-point displacement gauges to measure the displacement of surrounding rock at different depths, and bolt stress gauges to measure the radial stress.

The results of the multi-point displacement measurement in tunnel #1(K1 + 540 m) are shown in Fig. 26. The deformation of the internal surrounding rock generally occurs within 8 m, and the obvious deformation is at a depth of 2 m. In addition, the secondary excavation led to a disturbance effect on the surrounding rock. Because of the late installation of the displacement meters, the measured values are relatively low.

The results of the rock bolt stress in tunnel #1(K1 + 540 m) are shown in Fig. 27. The radial stress at the depth of 2 m on the right shoulder is larger than other points, and the maximum is about 400 MPa. The stress at the depth of 5 m on left shoulder is still about 40 MPa, indicating that the depth of deformation zone is more than 4 m, which agreed with the results of the multi-point displacement measurement.

4.4 Damage Modes

According to the observation of characteristics of soft rock during the excavation, the damage modes of tunnels can be classified as shotcrete layer fracture, steel arch distortion, collapse at the face, as shown in Fig. 28.
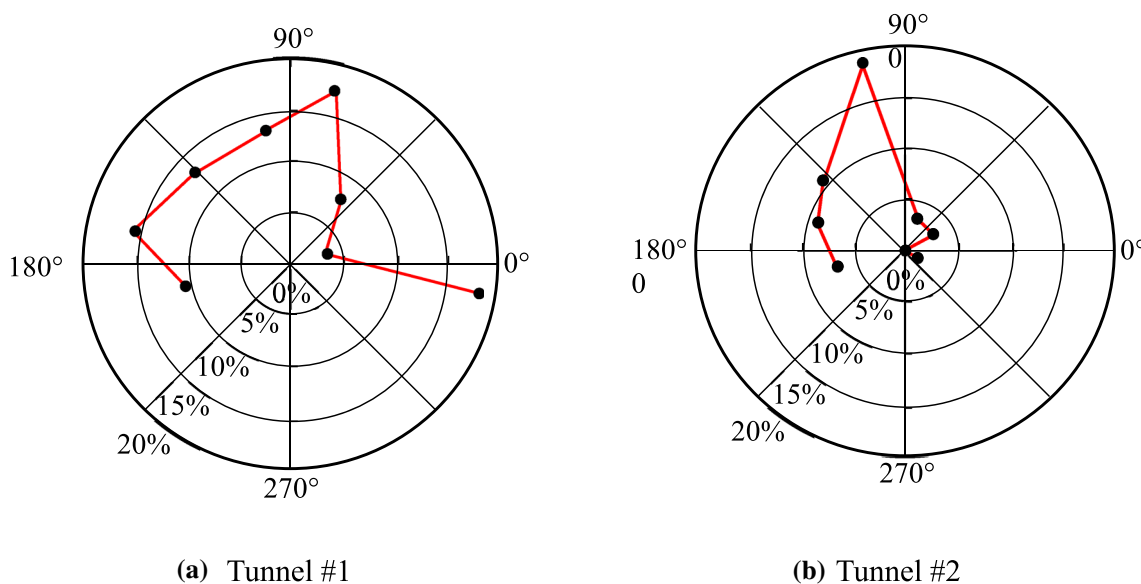
(a) Tunnel #1 **(b)** Tunnel #2

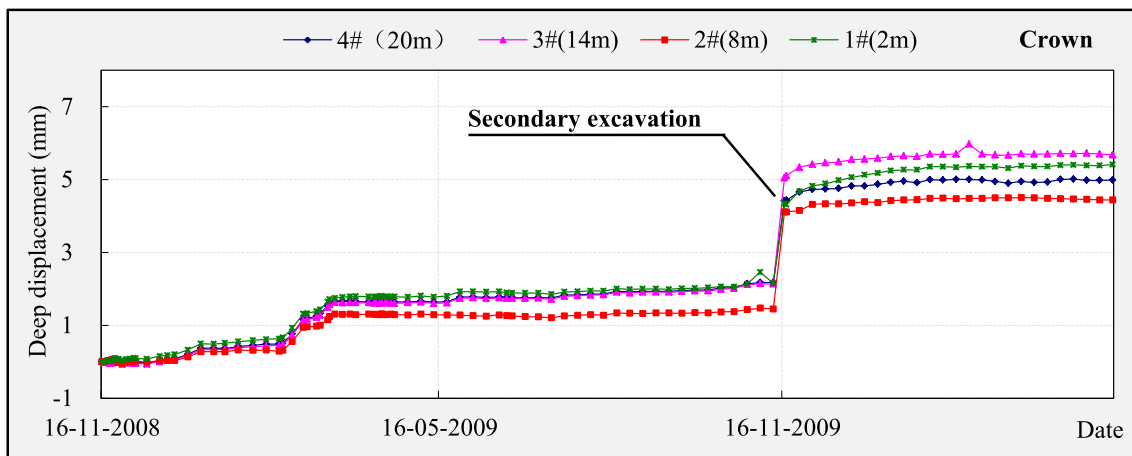**Fig. 25** The distribution of largest deformation position

Fig. 26 Deep displacement measurement

Figure 28a shows that separated shotcrete from the surface of surrounding rock at K1 + 660 m of Tunnel #1 occurred in left arch foot of tunnel, and the maximum separation width is more than 20 cm. There are some cracks at the bottom of the nearby left sidewall and these cracks have the characteristics of shear failure. Figure 28b shows the deformed steel arch in the corresponding location.

The tunnel face can be considered to be under uniaxial compression state, and the chlorite schist has a low compressive strength, which causes the face bulging inward. Once the installation of support structures is not timely, it is easy to result in the collapse at tunnel face. There were four large-scale collapses during the excavation of headrace tunnels. Figure 28c shows the collapse at K1 + 759 m of Tunnel #1, with a collapse volume of about $500 \sim 1000$ m^3. Additionally, this collapse was influenced by

chlorite schist stratification, which intensified the degree of inward bulge.

5 Measures and Suggestions

(1) Reserved deformation
Once preliminary supports cannot provide enough resistance forces (e.g., less than 2 MPa), the large deformation of soft rock will occur. Reserved deformation is an effective measure to avoid the intrusion for the large deformation of soft rock, and it can greatly release the ground stress and reduce the load on the preliminary support. Therefore, if the secondary lining is not considered, the best measure to ensure the designed cross
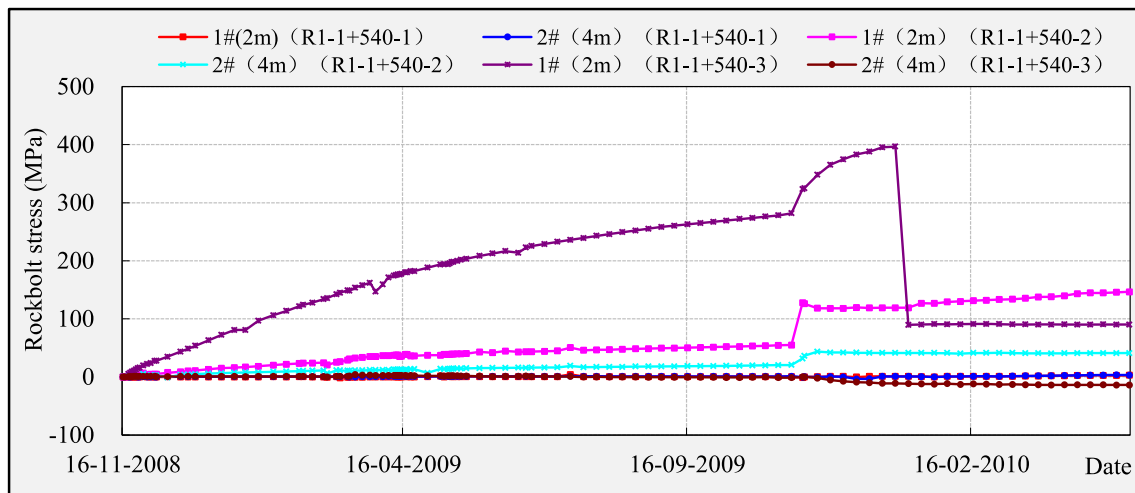
Fig. 27 Rockbolt stress measurement

(a) The separated shotcrete layer　　　　**(b)** The deformed steel arch　　　　**(c)** The collapse at the face

Fig. 28 Typical damage modes

section is the reasonable reserved deformation for soft rock.

(2)　Support structure

It is suggested that the lattice girder should be used in the construction of T1 stratum of the headrace tunnel, and the section I-shaped steel can be used to support the poor surrounding rock, such as chlorite schist. In addition, a long and short combined bolt is an effective support method. The short bolt constrains the surface part and does not loosen and fall off. The long bolt connects the shallow reinforcement ring and the deep part together to form a whole thick enough to meet the requirements of the stability of soft rock surrounding rock.

(3)　Support timing

Preliminary supports are not for controlling the formation of plastic zone, but for controlling the formation of loose zone and further development of plastic zone under the premise of stability of surrounding rock. This principle is the key to determining the timing of preliminary support.

For the soft surrounding rock, the plastic zone will continue to develop after the preliminary support, and begin to appear loose zone. When the radius of the loose zone is close to and will be equal to the reinforcement range composed of anchor net and surrounding rock, it is considered that the preliminary support has fully played its role. When the loose zone exceeds the zone of bolt reinforcement, the surrounding rock will be unstable, and at this time, it is the best time to carry out special support.

If the convergence deformation of surrounding rock is stable after the preliminary support and reinforcement support, it indicates that the preliminary support and reinforcement support have played a full bearing role and ensured the stability of the tunnel. The timing of the secondary lining support can be determined by referring to the relevant specifications and according to the on-site construction equipment and environment.

6 Conclusion

In order to resolve the large deformation problem of soft rock, this study conducted a series of laboratory tests and field monitoring tests, revealing the relationship between engineering properties of soft rock and performance under excavation of deep tunnel. The following conclusions are drawn:

(1) Based on the results of physical and chemical tests, the main mineral composition of soft rock is chlorite schist, and its structure is easy to be destroyed or weathered, especially after contacting water. The free swell rate of the rock samples is 10~25%, and the average swell force is 11 kPa, which indicated that the soft rock has a weak swell force. Therefore, effect of swell property is not the main factor of large deformation.

(2) Based on the results of a series of mechanical tests, it can be obtained that soft rocks are sensitive to confining pressure, and have an obvious strain hardening property. And the residual strength of the soft rock is more sensitive than the peak strength. The softening effect of soft rock is intensified at low confining pressure. After soft rock contacted water, the softening effect is obvious, whereas the hardening effect is weakened greatly. The elastic modulus of the saturated sample is not sensitive to the confining pressure, whereas the elastic modulus of dry sample is sensitive. The strength of soft rock declined dramatically due to the process of unloading and loading.

(3) The monitoring data shows soft rock has a rapid short-term deformation and a slow long-term deformation property, and its short-term deformation even reaches 10~20 cm. In addition, the phenomenon of "shrinkage" is prominent in the section of soft rock, and most deformations of surrounding rock exceed the tunnel clearance by 20~60 cm. For the mechanical state of internal surrounding rock, the deformation and stress generally occurs within 8 m, and the obvious location is the depth of 2 m. In addition, the damage modes of soft rock tunnels can be classified as shotcrete layer fracture, steel arch distortion, collapse at the face.

(4) The best measure to ensure the designed cross section is the reasonable reserved deformation for soft rock. In addition, I-shaped steel can be used for poorer soft rock. And the long and short combined bolts are an effective support method.

Declarations

Conflict of interest The authors declared that they have no conflicts of interest to this work. We declare that we do not have any commercial or associative interest that represents a conflict of interest in connection with the work submitted.

References

1. Wang, T.; Tan, L.; Xie, S.; Ma, B.: Development and applications of common utility tunnels in China. Tunn. Undergr. Sp. Technol. **76**, 92–106 (2018)
2. Zhang, J.R.; Wu, J.; Yan, C.W.; Gou, X.M.; Ye, L.; Feng, J.M.: Construction technology of super-large section of highway tunnels with four or more lanes in China. China J. Highw. Transp. **33**, 14–31 (2020)
3. Guo, W.; Zhu, D.: A review of the transient process and control for a hydropower station with a super long headrace tunnel. Energies **11**, 2994 (2018)
4. Shiyong, W.; Manbin, S.; Jian, W.: Jinping hydropower project: main technical issues on engineering geology and rock mechanics. Bull. Eng. Geol. Environ. **69**, 325–332 (2010)
5. Zhang, Z.; Shi, X.; Wang, B.; Li, H.: Stability of NATM tunnel faces in soft surrounding rocks. Comput. Geotech. **96**, 90–102 (2018)
6. Feng, G.L.; Feng, X.T.; Chen, B.R.; Xiao, Y.X.: Microseismic sequences associated with rockbursts in the tunnels of the Jinping II hydropower station. Int. J. Rock Mech. Min. Sci. **80**, 89–100 (2015)
7. Hoek, E.: Big tunnels in bad rock. J. Geotech. Geoenviron. Eng. **127**, 726–740 (2001)
8. Yang, Z.M.; Wu, S.C.; Gao, Y.T.; Jin, A.B.; Cong, Z.J.: Time and technique of rehabilitation for large deformation of tunnels in jointed rock masses based on FDM and DEM numerical modeling. Tunn. Undergr. Sp. Technol. **81**, 669–681 (2018)
9. Tu, X.B.; Jian, B.; Wang, S.J.; Bian, H.Y.; Wang, J.; Li, S.G.: Swelling behavior induced by alteration in granite and its implications on underground excavation. Tunn. Undergr. Sp. Technol. **20**, 378–389 (2005)
10. Zhang, H.; Chen, L.; Zhu, Y.M.; Zhou, Z.L.; Chen, S.G.: Stress field distribution and deformation law of large deformation tunnel excavation in soft rock mass. Appl. Sci. **9**, 865 (2019)
11. Zhao, G.Z.; Ma, Z.G.; Zhu, Q.H.; Mao, X.B.; Feng, M.M.: Roadway deformation during riding mining in soft rock. Int. J. Min. Sci. Technol. **22**, 539–544 (2012)
12. Meng, L.; Li, T.; Jiang, Y.; Wang, R.; Li, Y.: Characteristics and mechanisms of large deformation in the zhegu mountain tunnel on the sichuan-tibet highway. Tunn. Undergr. Sp. Technol. **37**, 157–164 (2013)
13. Yadav, S.; Saldana, C.; Murthy, T.G.: Experimental investigations on deformation of soft rock during cutting. Int. J. Rock Mech. Min. Sci. **105**, 123–132 (2018)
14. Terzaghi, K.: Rock defects and loads on tunnel supports. In: Proctor, R.V., White, T.L. (eds.) Rock Tunneling with Steel Supports, pp. 17–99. Commercial Shearing and Stamping Co., Youngstown (1946)
15. Egger, P.: Design and construction aspects of deep tunnels (with particular emphasis on strain softening rocks). Tunn. Undergr. Sp. Technol. **15**, 403–408 (2000)
16. He, M.C.; Li, G.F.; Liu, Z.: Countermeasures aiming at the support for crossing roadway of deeply buried soft rocks in Xing an coal mine. J. Min. Saf. Eng. **24**, 127–131 (2007)

17. Meng, B.; Jing, H.W.; Chen, K.F.; Su, H.J.: Failure mechanism and stability control of a large section of very soft roadway surrounding rock shear slip. Int. J. Min. Sci. Technol. **23**, 127–134 (2013)

18. Yang, F.; Zhang, C.; Zhou, H.; Liu, N.; Zhang, Y.; Azhar, M.U.; Dai, F.: The long-term safety of a deeply buried soft rock tunnel lining under inside-to-outside seepage conditions. Tunn. Undergr. Sp. Technol. **67**, 132–146 (2017)

19. Singh, B.; Goel, R.K.; Jethwa, J.L.; Dube, A.K.: Support pressure assessment in arched underground openings through poor rock masses. Eng. Geol. **48**, 59–81 (1997)

20. Huang, X.; Liu, Q.S.; Qiao, Z.: Research on large deformation mechanism and control method of deep soft roadway in Zhuji coal mine. Rock Soil Mech. **33**, 827–834 (2012)

21. Ulusay, R.: The ISRM Suggested Methods for Rock Characterization, Testing and Monitoring: 2007–2014. Springer, Cham (2014)

22. He, M.C.; Xie, H.P.; Peng, S.P.; Jiang, Y.D.: Study on rock mechanics in deep mining engineering. Chin. J. Rock Mech. Eng. **24**, 2803–2813 (2005)

23. Zhang, N.; He, M.; Liu, P.: Water vapor sorption and its mechanical effect on clay-bearing conglomerate selected from China. Eng. Geol. **141**, 1–8 (2012)

24. He, M.C.: Latest progress of soft rock mechanics and engineering in China. J. Rock Mech. Geotech. Eng. **6**, 165–179 (2014)

25. Diamantis, K.; Gartzos, E.; Migiros, G.: Influence of petrographic characteristics on physico-mechanical properties of ultrabasic rocks from central Greece. Bull. Eng. Geol. Environ. **73**, 1273–1292 (2014)

26. Johansson, E.: Technological Properties of Rock Aggregates. Luleå University of Technology, Luleå (2011)

27. Alonso, E.E., Ledesma, A.: Advances in understanding engineered clay barriers. In: Proceedings of the International Symposium on Large Scale Field Tests in Granite. CRC Press, Sitges (2005)

28. Kai, C., Jian-Qing, L., Peng, L.: Study on engineering properties of alteration zone in a tunnel project. In: 2011 International Conference on Electric Technology and Civil Engineering (ICETCE). pp. 2625–2627 (2011)

29. Manap, M.A.; Ramli, M.F.; Sulaiman, W.N.A.; Surip, N.: Application of remote sensing in the identification of the geological terrain features in Cameron Highlands, Malaysia. Sains Malaysa. **39**, 1–11 (2010)

30. Pappalardo, G.; Punturo, R.; Mineo, S.; Ortolano, G.; Castelli, F.: Engineering geological and petrographic characterization of migmatites belonging to the Calabria-Peloritani Orogen (Southern Italy). Rock Mech. Rock Eng. **49**, 1143–1160 (2016)

31. Zhang, G.; Chen, M.; Liu, X.; Zhao, W.; Pu, X.; Yu, N.: Relationship between rock compositions and mechanical properties of reservoir for low-permeability reservoirs. Pet. Sci. Technol. **31**, 1415–1422 (2013)

32. Bian, K.; Liu, J.; Liu, Z.; Liu, S.; Ai, F.; Zheng, X.; Ni, S.; Zhang, W.: Mechanisms of large deformation in soft rock tunnels: a case study of Huangjiazhai Tunnel. Bull. Eng. Geol. Environ. **78**, 431–444 (2019)

33. Lin, Z.H.; Xiang, W.; Zhang, Y.M.: Experimental research on influences of physical indices and microstructure parameters on strength properties of red stone from western Hunan. Chin. J. Rock Mech. Eng. **29**, 124–133 (2010)

34. Li, B.X.; Deng, J.H.: Experimental study of physico-mechanical properties of fault materials from Shenxigou rupture of Longmenshan fault. Chin. J. Rock Mech. Eng. **30**, 2653–2660 (2011)

35. Bai, C.; Xue, Y.; Qiu, D.; Su, M.; Ma, X.; Liu, H.: Analysis of factors affecting the deformation of soft rock tunnels by data envelopment analysis and a risk assessment model. Tunn. Undergr. Sp. Technol. **116**, 104111 (2021)

36. Wu, K.; Shao, Z.; Qin, S.; Zhao, N.; Chu, Z.: An improved nonlinear creep model for rock applied to tunnel displacement prediction. Int. J. Appl. Mech. **13**, 2150094 (2021)

37. Chu, Z.; Wu, Z.; Wang, Z.; Weng, L.; Liu, Q.; Fan, L.: Micromechanism of brittle creep in saturated sandstone and its mechanical behavior after creep damage. Int. J. Rock Mech. Min. Sci. **149**, 104994 (2022)

38. Chen, Z.J.; Wen, X.M.: Swelling rocks and stability of tunnels. Chin. J. Rock M ech. Eng. **1**, 1–10 (1983)

39. Anagnostou, G.: A model for swelling rock in tunnelling. Rock Mech. Rock Eng. **26**, 307–331 (1993)

40. Jiang, Y.; Yoneda, H.; Tanabashi, Y.: Theoretical estimation of loosening pressure on tunnels in soft rocks. Tunn. Undergr. Sp. Technol. **16**, 99–105 (2001)

41. Chu, Z.; Wu, Z.; Liu, Q.; Liu, B.; Sun, J.: Analytical solution for lined circular tunnels in deep viscoelastic burgers rock considering the longitudinal discontinuous excavation and sequential installation of liners. J. Eng. Mech. **147**, 4021009 (2021)

42. Goel, R.K.; Jethwa, J.L.; Paithankar, A.G.: Tunnelling through the young Himalayas—a case history of the Maneri-Uttarkashi power tunnel. Eng. Geol. **39**, 31–44 (1995)

43. Wu, K.; Shao, Z.; Sharifzadeh, M.; Chu, Z.; Qin, S.: Analytical approach to estimating the influence of shotcrete hardening property on tunnel response. J. Eng. Mech. **148**, 4021127 (2022)

44. Yu, K.; Ren, F.; Puscasu, R.; Lin, P.; Meng, Q.: Optimization of combined support in soft-rock roadway. Tunn. Undergr. Sp. Technol. **103**, 103502 (2020)

45. Guo, Z.; Wang, J.; Zhang, Y.: Failure mechanism and supporting measures for large deformation of Tertiary deep soft rock. Int. J. Min. Sci. Technol. **25**, 121–126 (2015)

46. Yang, S.Q.; Chen, M.; Jing, H.W.; Chen, K.F.; Meng, B.: A case study on large deformation failure mechanism of deep soft rock roadway in Xin'An coal mine, China. Eng. Geol. **217**, 89–101 (2017)

47. Yassaghi, A.; Salari-Rad, H.: Squeezing rock conditions at an igneous contact zone in the Taloun tunnels, Tehran-Shomal freeway, Iran: a case study. J. Rock Mech. Min. Sci. **42**, 95–108 (2005)